Proton-Proton Triple Scattering Parameters R and A at 213 Mev*

ALAN C. ENGLAND,† WILLIAM A. GIBSON,† KAZUO GOTOW, ERNST HEER, AND JOHN TINLOT
Department of Physics and Astronomy, University of Rochester, Rochester, New York

(Received May 18, 1961)

As a part of a program to determine the p-p scattering matrix at 213 Mev the triple-scattering parameters R and A have been measured at 30°, 40°, 50°, 60°, 70°, 80°, and 90° in the center-of-mass system. The results are compared with a phase-shift analysis by MacGregor and Moravcsik and with the predictions of the boundary condition model of Saylor, Bryan, and Marshak.

I. INTRODUCTION

DESPITE the fact that the proton-proton interaction at energies of a few hundred Mev has been intensively studied for the last ten years, it has been impossible until very recently to obtain a unique analysis and a clear understanding of the experimental results. Early attempts[1] to explain the observed nucleon-nucleon scattering phenomena by purely meson theoretical arguments and the less ambitious approaches of finding a phenomenological potential or a unique partial-wave analysis, were severely hampered by the lack of sufficient data. As a consequence of the development of the techniques of producing intense polarized proton beams, since 1954 a relatively large body of data from double- and triple-scattering experiments has been obtained. The problem of analysis, however, has always seemed rather formidable. For example, the first extensive study to include triple-scattering results at[2] 310 Mev yielded eight distinct phase-shift solutions which were acceptable on purely formal grounds.[3] Clearly it was very important to investigate the reasons for this great ambiguity. This has been done by a number of authors and we can now state unambiguously what experiments must be performed to arrive at a unique solution. If one describes the scattering process by means of the scattering matrix[4] and omits terms which violate invariance requirements, one sees that only five terms remain, whose ten complex coefficients are parameters to be determined by experiment. These coefficients, which are functions of the scattering angle, may be determined by one of the following three approaches:

(a) One determines the coefficients at one particular angle by measuring a sufficient number of experimental quantities at this particular angle. Since nine coefficients are to be determined (one phase is arbitrary), at least nine experiments must be performed. It appears[5] in fact that 11 precise experiments are required to ensure uniqueness of the solution. In practice experimental errors might increase the necessary number to more than that.

(b) One determines the scattering matrix over the complete angular range. In this case one may make use of the fact that the scattering matrix is unitary,[6] which imposes five conditions relating the imaginary part of the coefficients at one angle to integrals over the whole angular range. Five experiments performed over the angular range from 0° to 90° (c.m.) are then sufficient to determine the p-p scattering matrix uniquely. This procedure is however impractical unless one imposes restrictions on the dependence of the coefficients on the angle. This determines the minimum angular resolution required and the minimum number of points to be measured in the given angular range. Such a limitation is of course equivalent to choosing the highest order Legendre polynomial which contributes significantly to the angular distribution.

(c) One performs sufficient experiments to yield a unique phase-shift analysis. Since the unitarity requirement is automatically included, any five experiments which will determine the scattering matrix uniquely will also define a unique partial-wave solution.[7] In practice, in making a partial-wave analysis, one also assumes restrictions on the angular dependence of the experimental parameters, since one neglects states with angular momentum greater than a maximum defined by a quantum number $l_{\max}$. The choice of $l_{\max}$ puts a definite limit on the required angular resolution and detail of measurement. It is, however, well known that $l_{\max}$ must be at least 5 in order to explain data at energies of a few hundred Mev. The number of phase shifts to be determined is therefore quite large. In a modification of the usual phase shift analysis, which has been applied in several recent studies,[8] the contribution of the

* Work done under the auspices of the U. S. Atomic Energy Commission.

† Present address: Oak Ridge National Laboratory, Oak Ridge, Tennessee.

[1] Proton-proton scattering experiments and their analysis have been summarized in two recent review articles: R. T. N. Phillips, Repts. Progr. in Phys. **22**, 562 (1959); M. H. MacGregor, M. T. Moravcsik, and H. P. Stapp, Ann. Rev. Nuclear Sci. **10**, 291 (1960).

[2] O. Chamberlain, E. Segrè, R. D. Tripp, C. Weigand, and T. Ypsilantis, Phys. Rev. **105**, 288 (1957); James Simmons, *ibid.* **104**, 416 (1956).

[3] H. P. Stapp, T. J. Ypsilantis, and N. Metropolis, Phys. Rev. **105**, 302 (1957).

[4] L. Wolfenstein and J. Ashkin, Phys. Rev. **85**, 947 (1952); R. Dalitz, Proc. Phys. Soc. (London) **A65**, 175 (1952).

[5] C. R. Schumacher and H. A. Bethe, Phys. Rev. **121**, 1534 (1961).

[6] L. Puzikov, R. Ryndin, and Ia. Smorodinski, Soviet Phys.—JETP **5**, 489 (1957).

[7] R. E. Marshak, *Proceedings of the London Conference on Nuclear Forces and the Few-Nucleon Problem* (Pergamon Press, New York, 1960), p. 5.

[8] P. Cziffra, M. H. MacGregor, M. J. Moravcsik, and H. P. Stapp, Phys. Rev. **114**, 880 (1959); M. H. MacGregor, M. J. Moravcsik, and H. P. Stapp, *ibid.* **116**, 1248 (1959); M. H. Mac-

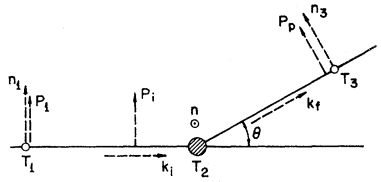

FIG. 1. Schematic diagram of the R geometry.

higher angular momentum states is attributed entirely to the one-meson exchange process. This reduces the number of phase shifts to be determined in an analysis of the experiments. By studying the behavior of the fitting parameter χ^2 as a function of the meson-nucleon coupling constant, one can rule out nonphysical solutions. Therefore the modified analysis will in general result in a smaller number of acceptable phase shift solutions.

The latter approach to the problem of analyzing the proton-proton interaction seems at present to be the most fruitful and is the one upon which we shall base our discussion. An experimental program has been under way for several years at the University of Rochester, the purpose of which is to complete five scattering experiments at 213 Mev, covering the angular range 0° to 90° (c.m.). These experiments include the measurement of the cross section $(d\sigma/d\omega)$, the polarization (P), and three of the triple-scattering parameters originally introduced by Wolfenstein[9] (R, A, and D). We report here on the measurement of the parameters R and A over the angular range 30° to 90° in the center-of-mass system. We shall compare our results to the predictions of the latest phenomenological potential models and describe an attempt at a partial-wave analysis which, though based on an incomplete set of data in the sense defined above, gives definite promise that a unique solution will soon be found.

II. TRIPLE SCATTERING PARAMETERS R AND A

Wolfenstein[9] first introduced the nomenclature which is now generally followed in writing the general expression for the polarization $\mathbf{P}_f$ produced by the scattering of protons with initial polarization $\mathbf{P}_i$ by an unpolarized target.

$$I\mathbf{P}_f = I_0\{[P+D\mathbf{P}_i\cdot\mathbf{n}]\mathbf{n}+[A\mathbf{P}_i\cdot\mathbf{k}_i+R\mathbf{P}_i\cdot\mathbf{s}_i]\mathbf{s}_f + [A'\mathbf{P}_i\cdot\mathbf{k}_i+R'\mathbf{P}_i\cdot\mathbf{s}_i]\mathbf{k}_f\}, \quad (1)$$

$$I = I_0(1+P\mathbf{P}_i\cdot\mathbf{n}). \quad (1a)$$

In these expressions $\mathbf{k}_i$ and $\mathbf{k}_f$ are unit vectors parallel to the momentum before and after the scattering: $\mathbf{n}=(\mathbf{k}_i\times\mathbf{k}_f)/|\mathbf{k}_i\times\mathbf{k}_f|$ is the normal to the scattering plane; $\mathbf{s}_i=\mathbf{n}\times\mathbf{k}_i$ and $\mathbf{s}_f=\mathbf{n}\times\mathbf{k}_f$ are unit vectors in the scattering plane normal to the momentum before and after the scattering; I and I_0 are the intensities for scattering of a polarized and unpolarized beam, respectively; P is the polarization which would be produced in scattering an unpolarized beam; and D, A, R, A', and R' are the triple scattering parameters. The latter are determined in triple scattering experiments which are usually performed as follows.

The circulating proton beam of a synchrocyclotron is scattered from an internal target T_1 in a plane specified by the unit normal vector $\mathbf{n}_1$. The scattered beam then has a transverse polarization $\mathbf{P}_1=P_1\mathbf{n}_1$. If the beam is magnetically deflected in a plane containing the vector $\mathbf{n}_1$, the polarization becomes partially longitudinal. It is thus possible, if desired, to change the direction of the polarization vector $\mathbf{P}_1$ relative to the beam direction. We therefore distinguish between $\mathbf{P}_1$ and the polarization $\mathbf{P}_i$ of the beam incident on the second scattering target.

The polarized beam is then scattered from a hydrogen target (T_2) in a plane specified by the unit normal vector $\mathbf{n}$. The second scattered beam has polarization $\mathbf{P}_f$, which is related to $\mathbf{P}_i$ by the expression of Eq. (1).

Finally, the second scattered beam is scattered from a target T_3 in a plane specified by the unit normal vector $\mathbf{n}_3$, and the relative scattered intensity to the "right" and "left" is measured. From the right-left asymmetry, one obtains a measure of the component of polarization along $\mathbf{n}_3$. Since $\mathbf{n}_3$ is usually chosen normal to the direction of the beam incident on T_3, this method only allows measuring a transverse component of polarization. It may therefore be necessary to interpose a spin-precession magnet between T_2 and T_3 so that a longitudinal component is changed to a transverse one. We therefore distinguish between the second scattered beam polarization $\mathbf{P}_f$ and the polarization $\mathbf{P}_p$ of the beam incident on T_3.

The third scattering apparatus, consisting of T_3 and the associated scintillation counters, is called the polarimeter. The right-left asymmetry in the third scattering is a function only of $\mathbf{P}_p$ and the analyzing power of the polarimeter $\mathbf{P}_3$

$$e=\mathbf{P}_3\cdot\mathbf{P}_p=P_3\mathbf{n}_3\cdot\mathbf{P}_p. \quad (2)$$

Different triple scattering geometries are used to obtain simple relations between the measured asymmetry e and a particular triple scattering parameter. We shall now describe the geometries we used in our measurement of R and A.

In the R geometry (Fig. 1), no spin-precession magnets are used so that $\mathbf{P}_i=\mathbf{P}_1$ and $\mathbf{P}_f=\mathbf{P}_p$. The second scattering plane is chosen so that $\mathbf{n}$ is normal to $\mathbf{P}_i$. The polarimeter is placed so that $\mathbf{n}_3=\mathbf{s}_f$. From Eqs. (1) and (2) it then follows that the measured asymmetry is given by

$$e_R=\mathbf{P}_3\cdot\mathbf{P}_p=\mathbf{P}_3\cdot\mathbf{P}_f=P_3\mathbf{n}_3\cdot[\mathbf{P}_n+RP_1\mathbf{s}_f]=RP_1P_3. \quad (3)$$

Gregor and M. J. Moravcsik, Phys. Rev. Letters 4, 524 (1960); G. Breit, *Proceedings of the London Conference on Nuclear Forces and the Few-Nucleon Problem* (Pergamon Press, New York, 1960); G. Breit, M. H. Hull, K. Lassila, and K. D. Pyatt, Jr., Phys. Rev. Letters 4, 79 (1960).

[9] L. Wolfenstein, Ann. Rev. Nuclear Sci. 6, 43 (1956).

In the A geometry (Fig. 2), a spin-precession magnet is introduced between T_1 and T_2, rotating the polarization $\mathbf{P}_1$ of the initial beam so that it makes an angle $(\pi-\chi)$ with the momentum vector and therefore has both a transverse and a longitudinal component. The second scattering plane is chosen so that $\mathbf{n}$ is normal to $\mathbf{P}_i$. With this choice, and scattering down, $\mathbf{P}_i=P_1\mathbf{s}_i \sin\chi-P_1\mathbf{k}_i \cos\chi$. The polarimeter is placed so that $\mathbf{n}_3=\mathbf{s}_f$, no magnet is between T_2 and T_3, and therefore $\mathbf{P}_p=\mathbf{P}_f$. From Eqs. (1) and (2) it follows that the observed asymmetry is given by

$$e_A=\mathbf{P}_3\cdot\mathbf{P}_p=\mathbf{P}_3\cdot\mathbf{P}_f=P_3\mathbf{n}_3\cdot[P\mathbf{n}-RP_1\mathbf{s}_f \sin\chi -AP_1\mathbf{s}_f \cos\chi]=-P_1P_3[R \sin\chi+A \cos\chi]. \quad (4)$$

In the calibration geometry (Fig. 3) the polarimeter is placed directly in the polarized proton beam. The energy of this beam is degraded to simulate the energy of the hydrogen-scattered beam (for a particular scattering angle). It is assumed that this process does not change the polarization, i.e., $\mathbf{P}_p=\mathbf{P}_1$. The normal to the plane of the polarimeter, $\mathbf{n}_3$, is chosen parallel to $\mathbf{n}_1$. From Eq. (2) it follows that the observed asymmetry is given by

$$e_C=\mathbf{P}_3\cdot\mathbf{P}_p=\mathbf{P}_3\cdot\mathbf{P}_1=P_3\mathbf{n}_3\cdot P_1\mathbf{n}_1=P_1P_3. \quad (5)$$

Combining Eqs. (3) and (4) with (5), we obtain the following equations for the desired triple scattering parameters in terms of the measured asymmetries:

$$R=e_R/e_C, \quad (6)$$

$$A=-(e_R \sin\chi+e_A)/e_C \cos\chi. \quad (7)$$

III. POLARIZED PROTON BEAM

A. Production of the Polarized Beam

The polarized beam is produced by scattering the internal circulating beam of the 3.3-m synchrocyclotron from a carbon target at about 15° (see Fig. 3). The beam emerges from the vacuum chamber through a thin aluminum window and passes through a quadrupole magnet and a "wedge" magnet, the exit of which limits the vertical extent of the beam to 3.8 cm. At a point about 75 cm beyond the edge of the "wedge" magnet poles, the beam has its smallest extent in the horizontal direction. A liquid hydrogen target is placed at this point for the R measurement and the point is denoted by $T_2(R)$. It is known from previous work[10] that the beam has a transverse polarization "up" and that the magnitude of this polarization (P_1) is 0.89±0.02. Note however that in these experiments it is not necessary to know this quantity, since it does not enter either of Eqs. (6) or (7).

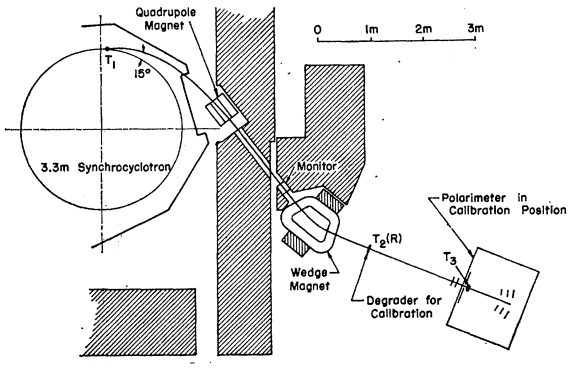

FIG. 3. The polarized proton beam and the polarimeter in the calibration geometry.

The energy of the beam was measured by taking integral range curves in poor geometry, and taking the mean range to be defined by the peak of the differential range curve, after correction for nuclear absorption. We find in this way that the mean range of the beam at the entrance to the hydrogen target is 44.5±0.7 g cm^{-2} of copper. The mean energy is therefore 217±2 Mev.[11] The width of the differential range curve at half maximum corresponds to an energy spread of 7 Mev. The incident protons lose about 8 Mev in traversing the hydrogen, so that the mean energy at the center of the target is 213±2 Mev.[11] The total spread in the energy is then about 15 Mev.

B. Beam Intensity Distributions at $T_2(R)$

As a prerequisite to precise alignment of the polarimeter [Sec. IV (D)], we required detailed knowledge of the beam-intensity distribution at the hydrogen target position. This was obtained by scanning the beam with a double scintillation telescope (called telescope A). The defining counter $A1$ had dimensions 0.32×0.32×0.32 cm and could be positioned reproducibly with an accuracy of better than 0.02 cm. Initial investigations revealed a small but noticeable low-energy component which (because of the dispersion of the magnetic system) caused the horizontal intensity profiles to appear somewhat asymmetric. Later measurements were performed with sufficient absorber in

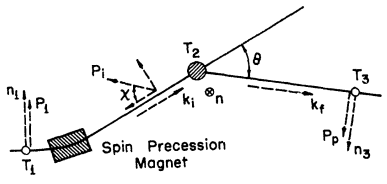

FIG. 2. Schematic diagram of the A geometry.

[10] W. G. Chestnut, E. M. Hafner, and A. Roberts, Phys. Rev. **104**, 449 (1956); E. M. Hafner, *ibid.* **111**, 297 (1958). Our beam geometry differs slightly from the one used in the above quoted experiments; a small deviation in beam polarization might therefore be expected which however does not affect our results.

[11] The energy has been computed from the range-energy curves of M. Rich and R. Madey, University of California Radiation Laboratory Report UCRL-2301 (unpublished); however, a correction has been applied to adjust for the currently accepted value of the mean excitation potential in copper $I=314$ ev (private communication by R. M. Sternheimer). In our preliminary report of the data we have quoted 210 Mev as the mean nominal energy compared to 213 Mev in this report. The earlier mean energy was based on the energy-range tables by R. M. Sternheimer, Phys. Rev. **115**, 137 (1959), which used the value $I=371$ ev.

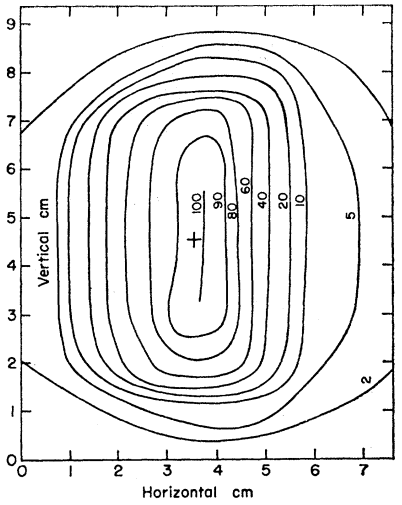

FIG. 4. Map of the proton beam at the $T_2(R)$ position. The cross indicates the calculated centroid of the intensity distribution.

the scanning telescope to assure the same range requirement as imposed by the polarimeter in the third scattering. Figure 4 shows a map of the beam in the plane normal to the beam direction at $T_2(R)$.

The centroid of the beam intensity distribution was calculated numerically and this point (marked by a cross in Fig. 4) was taken to define the effective center of the beam. Repeated measurements with fixed cyclotron operation conditions showed that the centroid could be defined to better than 0.10 cm horizontally, and 0.15 cm vertically.

C. Spin Precession Magnet

For the measurement of the parameter A, an additional magnet, which we shall call the spin-precession magnet, was used to produce a partially longitudinally polarized beam. The placement of the magnet and other components is shown in Fig. 5. The magnet was placed immediately after the wedge magnet with the plane of the poles vertical. The proton beam, after passing through the wedge magnet was thus deflected upwards by an angle ψ. This angle was calculated by numerical integration, using measured values of the field, and also measured directly by observing the shift of the beam. The result was $\psi=28°43'\pm3'$.

As is well known,[12] the polarization and momentum vectors precess at different rates because of the anomalous magnetic moment of the proton. The precession of the polarization relative to the momentum vector is given by

$$\xi=\gamma(\mu_p-1)\psi, \quad \text{where} \quad \gamma=(1-\beta^2)^{-\frac{1}{2}},$$

and μ_p is the proton magnetic moment in magnetons. The angle χ, appearing in Eqs. (4) and (7), is given by

$$\chi=\pi/2-\xi=26.7°\pm0.5°.$$

[12] A. Garren, Phys. Rev. **101**, 419 (1956); H. Mendlowitz, Ph.D thesis, University of Michigan, 1954 (unpublished).

The uncertainty in χ includes a contribution from the spread in energy of the proton beam.

D. Beam Intensity Distributions at $T_2(A)$

The hydrogen target, when used in the A geometry (Fig. 5), was placed 81 cm beyond the pole edge of the spin precession magnet. This position [which we call $T_2(A)$] was chosen to allow placing the protective slit S_{13} so that the polarimeter was shielded from the pole faces of the precession magnet. Beam intensity distributions were obtained using the scanning telescope described earlier. For mechanical reasons, we did not attempt to scan the beam in the plane transverse to the beam, but in a vertical plane containing the target center. The resulting beam map is shown in Fig. 6. Because of the dispersion of the magnet system, the distributions are markedly asymmetrical, and there is considerable correlation of energy with position. Thus there is some question as to whether in this case the centroid of the distribution really represents the effective beam center. This question will be discussed in connection with the general polarimeter alignment problem.

E. Beam Intensity Monitors

The primary monitor in data-taking runs was an air-filled ionization chamber which intercepted the proton beam as it entered the wedge focusing magnet (see Fig. 3). The current from the chamber was amplified and converted to a counting rate. As a secondary monitor we used the current from a large shielded air ionization chamber placed near the cyclotron. This chamber responded mainly to slow neutrons and usually served also as an indicator for use in adjusting the cyclotron.

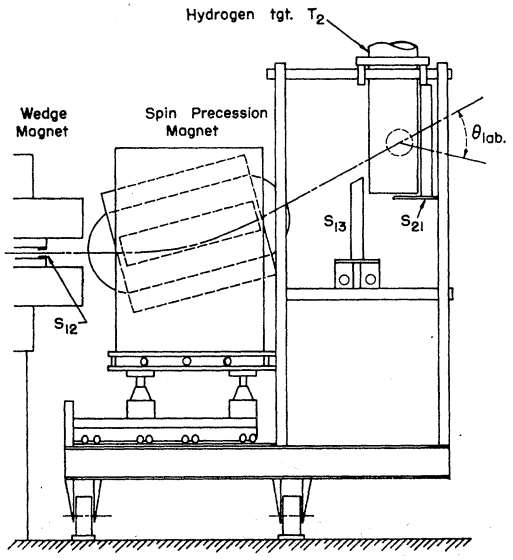

FIG. 5. Spin precession magnet and hydrogen target in the A geometry.

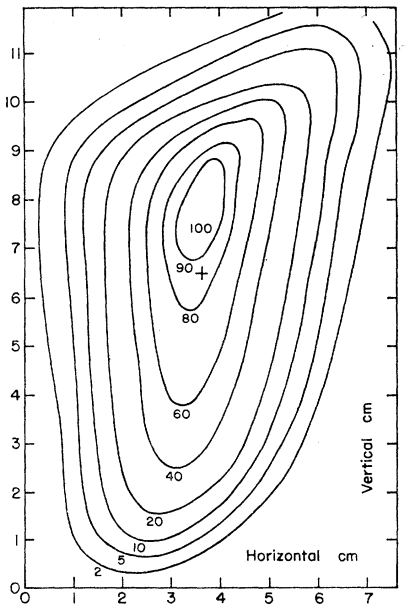

FIG. 6. Map of the proton beam at the $T_2(A)$ position. The cross indicates the calculated centroid of the intensity distribution.

F. Magnet and Cyclotron Settings

In the initial stages of the experiment we investigated the effect of varying the current in each magnet (including the main cyclotron magnet) upon the position of the beam at the hydrogen target. We thus established the requisite tolerance for each current setting to assure a negligible shift of the beam position.

We were somewhat concerned by the possibility that the beam composition and position might depend on the adjustment of cyclotron parameters, particularly those used to change the beam intensity. This is important because polarimeter calibration and beam distribution runs were usually taken at greatly reduced intensity. To check on any such effects, the beam intensity distribution at $T_2(R)$ was measured at full intensity with a small ionization chamber, and with x-ray film. The results were compared to those obtained with x-ray film and the scanning telescope A when the intensity of the cyclotron was reduced in the usual manner to 0.001 of maximum. No shift was found within the error of measurement ($\approx$0.2 cm). Of all the operating parameters which are usually varied, only one, the arc source position, was found to have an appreciable effect on beam position. Moving the arc source between its two extremes caused a shift of the centroid of the distribution by about 0.25 cm in the horizontal plane. We therefore take this as an upper limit on the possible change in beam position during a run.

To check for possible dependence of the mean energy of the beam upon the beam intensity, we compared the energy deduced from range measurements made on the hydrogen scattered beam (taken at maximum intensity) with that found from direct range measurements ($\approx$0.001 of maximum intensity). The two energies differed by less than 5 Mev.

G. Hydrogen Target

The hydrogen was contained in a cylindrical cup 12.5 cm long by 12.5 cm in diameter, with its axis perpendicular to the second scattering plane. The cylinder was made of 0.012-cm stainless steel, the ends of 0.32-cm brass. The hydrogen cup was mounted in an evacuated casing with stainless steel windows 0.005 cm thick and 7.6 cm wide. Since the beam incident on the target was appreciably narrower than the windows or the hydrogen cup (see Figs. 4 and 6), no scattering from the vacuum vessel or the end plates of the cup was to be expected. The cup was positioned by first locating it with respect to the casing when the target was open to the air, and then aligning the casing with respect to fiducial marks. We believe no appreciable error was introduced by distortions or shifts due to cooling. The hydrogen target was constructed so that the cup could be emptied of hydrogen by remote control for making background measurements.

IV. POLARIMETER

A. General Description

As discussed in Sec. II, the polarimeter is used to measure the right-left asymmetry e in the scattering of an incident beam in a plane defined by the unit normal vector $\mathbf{n}_3$.

The asymmetry [appearing in Eqs. (2) to (5)] is defined, as usual, by

$$e=(L-R)/(L+E), \tag{8}$$

where L and R denote the left and right scattered intensities. The polarimeter consists of detection counters, defining slits, and third-scattering target T_3. It is shown in schematic form in Fig. 7. A double scintillator telescope (called telescope II) detects the incident beam.

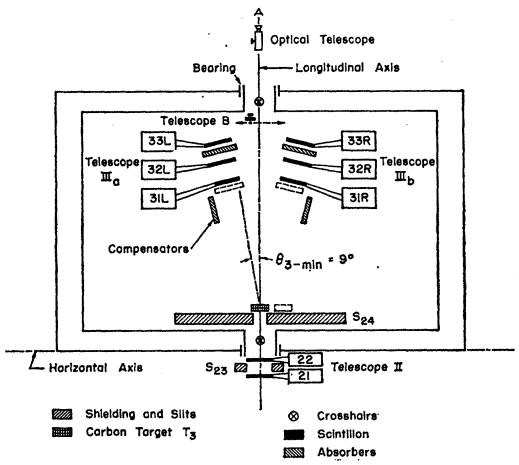

FIG. 7. The polarimeter.

TABLE I. Dimensions of counters and slits.

Slit	Counter telescope	Counter	Width (cm)	Height (cm)	Thickness (cm)
	II	21 and 22	7.53	11.42	0.32
	III_a and III_b	31	10.16	22.86	0.64
	III_a and III_b	32 and 33	12.70	25.40	0.64
	A	$A1$	0.32	0.32	0.32
	A	$A2$	2.54	2.54	0.32
	B	$B1$	0.64	19.10	0.64
	B	$B2$	2.54	21.60	0.64
S_{12}			[a]	3.8	5.08
S_{12}			[a]	$-5, +\infty$	5.82
S_{21}			7.53	[b]	5.82
S_{23}			8.90	[c]	6.35
S_{24}			6.40	10.16	5.82

[a] Appreciably wider than the beam.
[b] High enough to allow scattering over the entire angular range.
[c] Higher than beam.

Slit S_{24} defines the effective beam striking the carbon target T_3, since the II scintillators and the secondary slit S_{23} are large enough not to affect the beam definition. The distance from T_2 to T_3 was 203 cm, while the center of the slit S_{24} was about 5 cm from T_3. These distances, the dimensions of S_{24}, and the beam intensity distributions at T_2, determine the effective angular resolution. The results, obtained by numerical methods, is that the widths of the acceptance functions at half maximum are 2.7° in the second scattering plane and 1.8° in the third scattering plane. These widths (given in the laboratory system) are essentially independent of the scattering angle.

Two triple scintillator telescopes, denoted by III_a and III_b detect left and right scattered protons. The third scattering target, T_3, is of carbon and may be removed by remote control for making background measurements. Lucite compensating absorbers are automatically placed in front of the III telescopes when T_3 is retracted. The thickness of the compensators is chosen to provide the same stopping power as does T_3, so that the probability of detecting background particles entering slit S_{24} is not affected by the removal of T_3. Copper absorbers are placed between the second and third of the III telescope counters in order to set the desired threshold on the range of the third scattered protons. The relevant dimensions of counters and slits are given in Table I.

The electronic circuitry is simple and quite conventional and will not be described in detail. The II, III_a, and III_b coincidences are formed in separate coincidence circuits and recorded to give checks on operating conditions. They are then combined in double coincidence to form the V_a and V_b events. Random coincidences are measured when necessary by introducing 50 nanosec of relative delay between the II and III coincidence pulses.

The polarimeter is mounted on hollow bearings which clear the second scattered beam so that the polarimeter may be rotated by 180° about its symmetry axis (see Fig. 7), thus interchanging the III_a and III_b telescopes. The asymmetry e is calculated from the V rate of each telescope in the two positions of the polarimeter. We thus obtain two independent measurements of the asymmetry.

A pair of cross haris are placed inside each bearing and aligned on the symmetry axis and an optical telescope is aligned on the cross hairs. The polarimeter is then aligned optically by ensuring that the symmetry axis coincides with the effective second-scattering beam center line. The details of this procedure are given in Sec. IV (D).

B. Choice of Polarimeter Parameters

As mentioned in Sec. II, the polarimeter is characterized by the analyzing power P_3, which is a function of the energy of the incident beam. The analyzing power, however, depends on the particular choice of three parameters; the angular positions of the III telescopes, the target T_3 thickness, and the absorber thickness. One wants to maximize the analyzing power and at the same time obtain the highest counting rate. When these requirements conflict, a compromise must be made in the choice of the parameters. The dependence of the analyzing power upon the scattering angle was found to be rather insensitive, so the angle was chosen primarily to ensure small background counting rates (i.e., with T_3 out). Thus, as shown in Fig. 7, $\theta_{3\,\min}$ was set at 9°. The largest detected angle was then about 19°. The range of azimuth covered by each telescope varied from about ±45° at the minimum angle to about ±27° at the largest angle. The choice of T_3 thickness and absorber was then optimized at each hydrogen scattering angle. As the thickness of T_3 is increased, the scattered rate increases almost in proportion, but the analyzing power decreases because the average energy of protons scattered in T_3 decreases. Increasing the absorber thickness increases the analyzing power by eliminating inelastic scattering events, but decreases the counting rate because of nuclear absorption and scattering. The actual choice of T_3 was rather arbitrary, although we sacrificed analyzing power somewhat to obtain high counting efficiency. The absorber was chosen to coincide with

TABLE II. Polarimeter parameters.

Nominal c.m. scattering angle $\theta_{c.m.}$ (deg)	θ_{lab} (deg)	T_3 thickness (g/cm²)	Cu absorber in III telescopes (g/cm²)	Analyzing power $=P_3$ A telescope	Analyzing power $=P_3$ B telescope
30	14°16′	7.97	16.99	0.59±0.01[a]	0.60±0.01[a]
		(2.11)[b]		(0.62)[b]	(0.64)[b]
40	19°05′	7.97	15.63	0.55	0.56
50	23°53′	6.04	12.68	0.48	0.48
60	28°44′	3.93	11.32	0.42	0.43
		(1.60)[b]		(0.44)[b]	(0.48)[b]
70	33°37′	3.18	8.61	0.30	0.31
80	38°33′	2.11	5.66	0.22	0.21
90	43°31′	1.60	2.72	0.13	0.14
		(1.07)[b]		(0.13)[b]	(0.17)[b]

[a] The error is taken to be 0.01 for all points, although the statistical error is usually considerably smaller [see Sec. IV (C)].
[b] Thinner targets were used in the very first run in the R geometry. Correspondingly higher analyzing powers P_3 were obtained.

the "knee" of the range curve, i.e., the value of absorber beyond which the counting rate dropped steeply. The selected values of T_3 and absorber thickness are listed in Table II.

C. Calibration of the Polarimeter

After having chosen the polarimeter parameters, we proceeded to calibrate the polarimeter, i.e., measure $e_C = P_1 P_3$ for each angle of hydrogen scattering. This entailed simulating the hydrogen-scattered beam both as to spatial distribution at the target T_3 and as to the mean energy.

First let us consider the spatial distribution of the beam. In the actual scattering experiment, the intensity of protons accepted by slit S_{24} is not exactly uniform over the area of the slit. First the intensity varies slightly in a direction perpendicular to the polarimeter scattering plane because of the change in cross section with scattering angle. However, since the cross section in the laboratory frame varies almost as the cosine of the angle, the greatest variation (at $\theta_{\text{c.m.}}=90°$) only amounts to 6%. Since the polarimeter analyzing power should not depend at all critically on this variation, we did not attempt to simulate it during the calibration runs. We may also expect a slight variation in intensity in a direction along the polarimeter scattering plane because of the dependence of the hydrogen scattering cross section on polarization. We obtain from Eq. (1a)

$$I = I_0(1+P\mathbf{P}_i\cdot\mathbf{n}) = I_0(1+PP_i\cos\phi). \qquad (9)$$

In both the R and A geometry the second scattering is in the plane of the initial polarization. Therefore ϕ is nearly 90°. The width of S_{24} (6.35 cm) corresponds to $\Delta\phi=7°$ at $\theta_{\text{c.m.}}=30°$, and decreases to a minimum of $\Delta\phi=2.5°$ at $\theta_{\text{c.m.}}=90°$. Evaluating the effect at 30° (taking $P_1=0.90$ and $P_2=0.25$), one finds an intensity variation across the slit of 2.8%. We have calculated the asymmetry produced by this variation and found it to be 0.003 for the R geometry at 30° and smaller for all other angles and for the A geometry. We have therefore neglected this effect.

The alignment of the polarimeter for calibration was straightforward: Beam intensity distributions were measured at $T_2(R)$ and at a distance 195 cm further, and the beam center line was defined by the centroids of the two distributions. The polarimeter symmetry axis was then placed on this line with T_3 at a distance of 203 cm from the $T_2(R)$ position (see Fig. 3). In place of the hydrogen target, however, we introduced a series of lead absorbers (which we shall call degraders) which simulate the energy loss of protons scattering from hydrogen. A high Z material was chosen for the degraders so that Coulomb scattering would provide a nearly uniform intensity distribution at slit S_{24}. The variation in intensity when using the thinnest degrader (for smallest simulated hydrogen scattering angle) is then only a few percent. No attempt was made to correct for this.

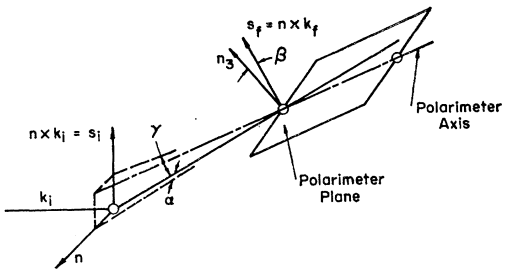

FIG. 8. The three types of misalignment of the polarimeter.

The degrader thicknesses were initially chosen from computations using standard range tables. However, a direct comparison of range in copper of degraded and hydrogen scattered protons showed that a sizeable error had been made, for reasons which are not completely understood. The ranges were therefore "matched" by adding appropriate thicknesses of copper to each degrader.

The measured analyzing powers at the nine angles from 30° to 90° (c.m.) are listed in Table II for the A and B telescopes separately.

We measured the variation of polarimeter analyzing power with small changes in energy of the protons. The result was that $\Delta P_3/\Delta R \leq 0.01$, where ΔP_3 is the change in analyzing power resulting from a change in range ΔR of g cm^{-2} of copper. Since we were able to match the ranges of degraded and hydrogen scattered protons to considerably better than 1 g cm^{-2} of copper, no appreciable error was introduced.

We also measured, in the calibration geometry, the sensitivity of the polarimeter to misalignment of a particular type; rotation of the polarimeter about an axis perpendicular to the scattering plane and passing through T_3. As will be shown later, this form of misalignment is by far the most important one. We shall denote the angle between the polarimeter and beam center-line axes by α (see Fig. 8). The misalignment sensitivity (the change in measured asymmetry per unit angle α) was thus found to be 0.002 ± 0.0003 per minute, for all hydrogen scattering angles. The magnitude of the alignment problem was clearly defined by this number. Since we expected to obtain statistical errors in the asymmetries of 0.01 or less, we evidently had to assure alignment with a precision for α of a few minutes at most. We believe the alignment error in the calibration geometry was insignificant. The quoted error of 0.01 for each value of P_3 in Table II is an estimate of the maximum uncertainty resulting from inexact matching of the range, spin-dependent scattering and depolarization effects in the degrader, alignment errors, and effects due to the intensity variation of the incident beam over the entrance slit S_{24} of the polarimeter.

D. Alignment of the Polarimeter

The problem of deciding upon the best method of aligning the polarimeter was a critical one because of

TABLE III. Discrepancy in alignment by methods I and II, expressed in terms of the angle α, as defined in Fig. 8 and the text.

Geometry	Nominal c.m. scattering angle (deg)	α (min)
Calibration	30	+2.7
	60	+0.2
	90	−0.1
R parameter	30	+1.0
	60	+1.6
	90	+2.9
A parameter	30	0
	40	−0.6
	50	0
	60	−2.6
	70	−1.2
	80	+6.0
	90	+2.4

the very high degree of accuracy required. In principle one merely set the polarimeter so that its symmetry axis coincides with the mean direction of the hydrogen-scattered beam. In practice one must take carefully into account many effects, the principle ones being: (a) the finite dimensions of the irradiated volume of the hydrogen target and of the area of the defining slit S_{24}, (b) the energy spread in the beam, particularly any correlation with the point of scattering in the hydrogen, and (c) the deflection of the scattered protons in the fringing field of the cyclotron. Other effects of minor importance will be mentioned in Sec. VI. In attempting to understand effects such as those above, we developed two different procedures of alignment, both of which were studied in detail under a variety of conditions. In the first (method I) we defined the effective beam center line by two points in space; the effective center of the incident beam at the hydrogen target position and the geometrical center of slit S_{24}. The second method (method II) resembles more closely that used by other experimenters.[2,13] We align the polarimeter on the line passing through the center of slit S_{24} and through the center of the beam intensity distribution at some distance *beyond* the slit. We expect the two methods to agree. The results showed slight discrepancies, which, however, we do not consider significant. These are discussed also in Sec. VI. We now describe these alignment procedures in detail.

In method I we follow a sequence of three steps. (1) We determine the effective beam center at the hydrogen target position $T_2(R)$ and 195 cm further along the beam by the method described in Sec. IIIB. (2) We place the polarimeter for the desired scattering angle $\theta_{\text{c.m.}}$. This requires that the polarimeter axis be in a vertical plane (second-scattering plane) containing the beam line found in step (1), that the axis be inclined by the angle θ_{lab} with respect to the incident beam line, and that the normal to the third scattering plane also be in the vertical plane containing the incident beam line. (3) We correct the alignment to account for the deflection of the scattered protons by the fringing magnetic field of the cyclotron. In order to do this we measured the component of fringe field normal to the scattered beam center line and computed the deflection of protons having the mean energy. This deflection was translated into an effective displacement of the beam center at the hydrogen target from that measured in step (1). The polarimeter was then realigned so that its axis passed through the displaced (or virtual) beam center. The fringe field was found to be equal to or less than 30 gauss and the virtual center was displaced from 0.25 cm to 0.40 cm from the actual center.

In method II the hydrogen target was in place and the polarimeter was placed approximately correctly (say by an abbreviated version of method I) at one of the desired angles of hydrogen scattering. We then investigated the beam intensity distribution in a region 90 cm beyond the center of slit S_{24}, using a double scintillation counter telescope (telescope B) whose defining counter $B1$ had dimensions 0.69×19.10 cm and a thickness of 0.32 cm; a copper absorber sets the same range threshold as is imposed by the polarimeter. The long dimension of the telescope was placed perpendicular to the polarimeter scattering plane, and the telescope was moved across the beam (see Fig. 7). The polarimeter was said to be aligned[14] when its axis coincided with the line passing through the center of S_{24} and the centroid of the distribution found with telescope B. A misalignment according to this criterion was corrected by rotating the polarimeter about an axis perpendicular to the third scattering plane and passing through the center of S_{24}. After the correction, the alignment was checked once again by another measurement of the intensity distribution with telescope B.

In comparing the two methods, one finds that they are largely equivalent; however, one can raise some objections to method I which are eliminated by method

TABLE IV. Typical counting rates in R geometry at 60° c.m. scattering angle, expressed in counts per minute. The symbols for the different types of counts are defined in the text. III and V rates are given for the average of A and B telescope, the two telescopes giving numbers which are identical within statistics.

Coincidence	T_2 full T_3 in	T_2 full T_3 out	T_2 empty T_3 in	T_2 empty T_3 out
II	7×10^4	7×10^4	2.4×10^4	2.4×10^4
III (left)	200	187	68	91
III (right)	360	248	161	129
V (left)	49	3.6	2.2	0.1
V (right)	44	4.1	2.1	0.3
V (left randoms)	0.4	0.0	negligible	negligible
V (right randoms)	0.2	0.4	negligible	negligible

[13] C. F. Hwang, T. R. Ophel, E. H. Thorndike, and R. Wilson, Phys. Rev. **119**, 352 (1960).

[14] One must account for the deflection of the protons by the fringe field in the region between slit S_{24} and the B telescope. However this effect was small and almost exactly compensated by the deflection of protons after scattering from the polarimeter target T_3, in the region between T_3, and the defining counter of the III telescopes.

TABLE V. Results in the R geometry. The indicated errors in e_R are statistical. R was computed for each run by averaging the ratio e_R/e_C found with each telescope. The indicated error in R includes an experimental error of 0.006 combined in the square with the statistical error in e_R. The values of R in the last column are the weighted averages of the results from different runs. The uncertainty in corrected c.m. scattering angle is estimated as explained in Sec. VI(C).

Nominal c.m. scattering angle	Corrected c.m. scattering angle	Run	e_R (A telescope)	e_R (B telescope)	$R=e_R/e_C$ (each run)	R (average)
30°	30°01′±30′	1	−0.136±0.027	−0.118±0.027	−0.202±0.032	−0.203±0.012
		2	−0.126±0.013	−0.120±0.013	−0.213±0.019	
		3	−0.107±0.013	−0.116±0.013	−0.193±0.019	
40°	40°05′	1	−0.061±0.015	−0.093±0.015	−0.145±0.024	−0.133±0.017
		2	−0.072±0.015	−0.058±0.015	−0.122±0.024	
50°	50°03′	1	−0.040±0.013	−0.013±0.013	−0.056±0.023	−0.041±0.018
		2	−0.018±0.015	−0.002±0.015	−0.021±0.028	
60°	60°04′	1	+0.008±0.029	+0.008±0.029	+0.018±0.050	+0.071±0.026
		2	+0.070±0.015	+0.008±0.015	+0.090±0.030	
70°	70°04′	1	+0.038±0.014	+0.049±0.014	+0.141±0.039	+0.147±0.029
		2	+0.057±0.015	+0·038±0.015	+0.153±0.042	
80°	80°04′	1	+0.060±0.018	+0.052±0.018	+0.250±0.062	+0.248±0.042
		2	+0.085±0.017	+0.024±0.017	+0.245±0.058	
90°	90°03′	1	+0.050±0.020	+0.019±0.020	+0.255±0.100	+0.223±0.055
		2	+0.034±0.019	+0.029±0.019	+0.218±0.097	
		3	+0.037±0.017	+0.021±0.017	+0.203±0.090	

II. Perhaps the most questionable assumption of method I is that the effective beam center at the hydrogen target really coincides with the centroid of the distribution in a vertical plane containing the target center. Pronounced correlations of energy with position, kinematic effects which vary over the volume of the target, and scattering of the beam in the air and from the slits, may change the effective direction of the second-scattered beam, and thus introduce spurious asymmetries. Although we believe that the contributions of such effects are all very small, we note that they are largely eliminated by the use of method II, since one examines the actual beam of protons accepted by slit S_{24}. The measurements obtained with method II, however, are of somewhat limited accuracy because of statistical fluctuations (because of small counting rate in telescope B). There is also the possibility of appreciable errors because of mechanical distortion and shift of counter telescope B. For example, a misalignment angle α of 1 min represents a displacement of the beam center at the telescope B position of only about 0.025 cm. We therefore do not consider as significant a disagreement between the two methods of less than 3 min of angle. In Table III we give a summary of the discrepancy between the two methods under the different conditions of measurement, expressed in terms of angular misalignment α as previously defined. We find that in all but one case, which is somewhat suspect for other reasons, the discrepancy corresponds to less than 3 min, which in turn corresponds to a change in asymmetry of 0.006. Since during most of the experiment we used method I for aligning the polarimeter, we have chosen to consider it the standard. However, we conclude from considerations such as those discussed above, that it is reasonable to include in the errors in asymmetry a contribution from experimental error of 0.006. This will be discussed further in Sec. VI.

E. Background Subtraction

In data-taking runs we measured the V_a and V_b counting rates with all possible permutations of the following conditions; with the hydrogen target full and empty, polarimeter frame in normal and inverted positions, polarimeter target T_3 in and out (but always with the Lucite compensator out and in), and with normal or added delay between the II and III coincidence pulses. Typical rates [these for the R geometry at 60° (c.m.)] are shown in Table IV. The counting times (monitor totals) were adjusted to be approximately proportional to the square roots of the rates in order to minimize the total running time; however, the time of the longest individual run was not allowed to exceed about 20 min in order to minimize the effects of drifts in the coincidence circuitry.

V. RESULTS

A. Triple Scattering Parameter R

Measurements in the R geometry were made in three separate runs extending over a period of about a year. The calibration of the polarimeter was also repeated several times including once after the completion of the measurement of the A parameter. The resulting values of e_R and $R=e_R/e_C$ are listed in Table V.[15] Note that measurements were performed at least twice at each of

[15] A. England, W. Gibson, K. Gotow, E. Heer, J. Tinlot, and R. Warner, *Proceedings of the 1960 Annual International Conference on High-Energy Physics at Rochester* (Interscience Publishers, Inc., New York, 1960); the data presented at this conference were preliminary, and differ slightly from those given here.

TABLE VI. Uncorrected results in the A geometry. The errors in e_A are statistical. α is the equivalent angle of misalignment, as defined in the text and illustrated in Fig. 8; Δe is corresponding correction to the asymmetries. The uncertainty in corrected c.m. scattering angle is estimated as described in Sec. VI (C).

Nominal c.m. scattering angle	Corrected c.m. scattering angle	Run	e_A (A telescope)	e_A (B telescope)	α (min)	Δe
30°	30°01′±30′	1	+0.262±0.020	+0.255±0.020	+5.9	+0.012
		3	+0.247±0.014	+0.287±0.014	0	0
40°	40°05′	1	+0.200±0.015	+0.171±0.015	+5.6	+0.011
		3	+0.206±0.014	+0.159±0.014	−0.6	−0.001
50°	50°03′	1	+0.075±0.018	+0.083±0.018	+6.0	+0.012
		2	+0.118±0.015	+0.161±0.015	+1.8	+0.004
		3	+0.085±0.013	+0.114±0.013	0	0
60°	60°04′	1	+0.016±0.022	+0.027±0.022	+6.4	+0.013
		2	+0.013±0.020	+0.021±0.020	+2.2	+0.004
		3	+0.022±0.015	+0.026±0.015	−0.7	−0.0
70°	70°04′	1	−0.004±0.021	−0.025±0.021	+6.6	+0.013
		2	−0.026±0.020	−0.021±0.020	+2.4	+0.005
		3	−0.024±0.015	−0.025±0.015	−2.3	−0.005
80°	80°04′	1	+0.011±0.031	−0.039±0.031	+6.8	+0.014
		2	−0.039±0.017	−0.006±0.017	+2.6	+0.005
		3	−0.019±0.018	+0.001±0.018	+4.6	+0.009
90°	90°03′	2	−0.010±0.017	+0.012±0.017	+2.8	+0.006
		3	+0.004±0.017	+0.005±0.017	+2.6	+0.005

the seven nominal angles 30°, 40°, 50°, 60°, 70°, 80°, and 90°. The effective mean angles of scattering are shown in the second column [see Sec. VI (C)]. The data obtained with the A and the B telescopes were treated independently and then averaged. As expected from the fact that the two telescopes are nearly identical, the asymmetries measured with each are statistically indistinguishable. Since the alignment procedure of method I was used for all of these runs, no alignment corrections were needed. Columns four and five of Table V show the results including statistical errors only. In columns six and seven the errors have been computed by combining in the squares the statistical error and an experimental error in e_R of 0.006, as indicated in Sec. IV (D) and discussed in Sec. VI. The result is also shown in Fig. 9.

B. Triple Scattering Parameter A

The measurements in the A geometry were also performed in three separate runs, but the combination of the results is complicated by the fact that different alignment procedures were followed in each run. We thus must correct each result to that corresponding to using the standard procedure of method I [see Sec. IV (D)]. Inasmuch as the corrections are in all cases relatively small, they can reasonably be done by assuming the spurious asymmetry introduced by a misalignment to be proportional to the angle of misalignment defined previously. The correction is then computed from the known sensitivity to misalignment: $\Delta e = (0.0020 \pm 0.0003)\alpha$, where α is given in minutes. The uncorrected values of the asymmetries e_A are given in columns 4 and 5 of Table VI for the A and B telescopes separately. The errors given are purely statistical. The angles α of "misalignment" in each case are listed in column 6. These angles were determined as follows:

In run 1 the alignment was performed following method I. It was discovered after the completion of this run that the determination of the beam center at the hydrogen target position had been performed with an incorrect range threshold. A comparison of the beam intensity distributions with the correct and incorrect absorbers showed that this resulted in a constant misalignment of 4.2±1.4 min at every angle of hydrogen scattering. We also found that the correction for deflection in the fringe field of the cyclotron had been incorrectly done, producing a misalignment varying from about 1.8 to 2.8 min.

In run 2, the alignment was performed following method I. The correct range threshold was used, but

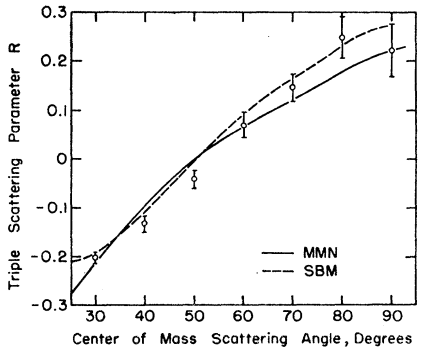

FIG. 9. The result of the R measurement at 213 Mev, compared with phase-shift solution b of reference 29 (M.M.N.) and the boundary condition model prediction of reference 27 (S.B.M.).

again the magnetic deflection correction was incorrect; the resulting misalignment varied from 1.8 to 2.8 min.

In run 3, exhaustive studies of the two alignment methods were conducted. We had, however, not yet decided upon the merits of each method and in fact chose an alignment which was intermediate. Correction to the alignment as required by method I was then equivalent to misalignment angles of 0 to 4.6 min.

The values of e_A in Table VI were thus corrected and averaged, with the exception that the point at 50° in run 2 was discarded. This will be discussed further in Sec. VI. The result for e_A/e_C, after averaging the results from the A and B telescopes, is shown in column 3 of Table VII[15]; the errors here again include an experimental error of 0.006, combined with the statistical errors in the square as in the treatment of the R data. Although the ratio e_A/e_C is the proper quantity to use in making the final analysis of the data, the calculation of A may be of use in comparing our results to published theoretical work. Since, as shown in Eq. (7), e_A/e_C is related to both of the parameters R and A, we must use the results of the R measurement to compute A. The result is given in column 4 of Table VII and in Fig. 10. We have assumed here that the errors in R and e_A/e_C are independent.

VI. ERRORS

A. Alignment Errors

Although there are very many effects which are equivalent to misalignment of the polarimeter they can be grouped into three types, each type corresponding to rotation of the polarimeter through a different angle α, β, or γ as illustrated in Fig. 8. The first form of misalignment (type α) is the one which we have been considering in the previous sections: a rotation of the polarimeter by an angle α around an axis $\mathbf{n}_3$, normal to the polarimeter plane. Misalignment of type β corresponds to rotation of the polarimeter about its symmetry axis, so that $\mathbf{n}_3$ makes an angle of $(90°-\beta)$ with the second-scattering plane. Finally, misalignment of type γ means that the polarimeter has been rotated by an angle γ around an axis $\mathbf{n}$ perpendicular to the second scattering plane. We have already noted the appreciable sensitivity of the asymmetry to changes in α. By contrast, we estimate that a misalignment in β or γ or 1 min would give at most a false asymmetry of $\Delta e=0.00015$ and 0.000025, respectively, illustrating the minor importance of misalignment of types β and γ,

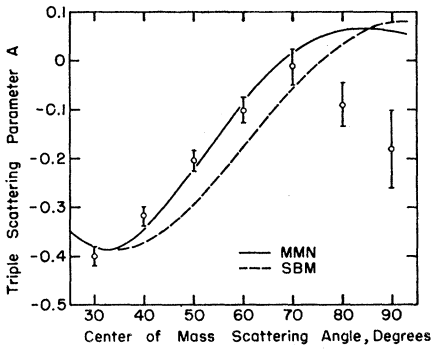

FIG. 10. The result of the A measurement at 213 Mev, compared with the phase-shift solution b of reference 29 (MMN) and the boundary condition model prediction of reference 27 (SBM).

TABLE VII. Corrected values of e_A/e_C, and the corresponding values of A. The results from the A and B telescopes have been averaged, and an experimental error of 0.006 is included in the error in e_A.

Nominal c.m. scattering angle	Corrected c.m. scattering angle	e_A/e_C	A
30°	30°01′±30′	+0.449±0.016	−0.400±0.019
40°	40°05′	+0.343±0.015	−0.317±0.019
50°	50°03′	+0.202±0.017	−0.205±0.021
60°	60°04′	+0.059±0.018	−0.102±0.025
70°	70°04′	−0.053±0.029	−0.012±0.036
80°	80°04′	−0.032±0.036	−0.090±0.046
90°	90°03′	+0.060±0.064	−0.180±0.077

We list below a number of possibly significant effects, and the corresponding types of misalignment which they produce.

(a) Precision, stability, and reproducibility of positioning the polarimeter. We believe, from repeated observations, that errors due to inaccurate positioning of the polarimeter, mechanical instability, and changes in the position of the beam center at T_2 during the run, correspond to $\alpha\leq 3$ min, and β, $\gamma\leq 15$ min.

(b) Positioning of hydrogen target. Because of the size of the target and its cylindrical geometry, the results are very insensitive to the exact location of the target cup. We expect no appreciable alignment error from this cause.

(c) Variation of the hydrogen cross section with angle. Since the cross section decreases with increasing angle, there is a bias favoring the detection of small-angle scattering events. This results in a vertical shift in the effective beam center, and thus a misalignment of type γ. We have estimated that γ is smaller than one minute of arc. The effect on the asymmetry is therefore negligible.

(d) Range threshold set by the polarimeter absorbers. The choice of absorbers to be placed in the III telescopes was made on the basis of obtaining good analyzing power. This required choosing a range threshold near the "knee" of the range curve, making the polarimeter counting rates rather sensitive to small changes in scattered proton energy. Two effects tend to cause correlation of energy loss with position in the target: the variation of energy with scattering angle causes the polarimeter to favor protons scattered through small angles; the amount of hydrogen which each proton traverses after scattering depends on both the position in the target and the scattering angle, but in sum favors the detection of protons scattering through large angles.

TABLE VIII. Phase shift sets at 210 Mev.[a] (1) Results of a nine-parameter search by MacGregor and Moravcsik[b] using calculated one-meson exchange contribution for G and higher partial waves. (2) The 210-Mev solution obtained with the boundary condition model by Saylor, Bryan, and Marshak.[c] The phase shifts are nuclear bar angles in degrees.

Phase shift set	$^1S_0$	$^1D_2$	$^3P_0$	$^3P_1$	$^3P_2$	ϵ_2	$^3F_2$	$^3F_3$	$^3F_4$	ϵ_4	$^3H_4$
(1)	6.3	7.4	−0.4	−20.8	16.9	−2.1	−0.1	−2.2	0.6	...	...
(2)	5.3	7.6	−0.6	−21.6	17.0	−2.8	1.7	−3.0	3.4	−1.3	0.2

[a] The computations were performed for 210 Mev, whereas our best estimate of the mean energy is now 213 Mev. See reference 11.
[b] See reference 15.
[c] See reference 27.

Both of these effects cause a misalignment of type γ, the size of which we have estimated to be smaller than one minute of arc. The effect on the asymmetry is again negligible.

(e) Spin dependent scattering of protons in air and scintillator telescope II. The only appreciable effect would be of type α. Rough calculations, as well as comparison of alignment methods I and II, show such scattering to be of negligible importance.

According to the above discussion, only type α misalignment introduces an error large enough to be taken into account. We therefore assume an experimental error due to misalignment of $\Delta e = \pm 0.006$. Since the various reasons for this error are assumed to occur in a random fashion, we combine the alignment error and the statistical error in the squares to give the final error quoted in Tables V and VIII and shown in Figs. 9 and 10.

B. Uncertainty in Direction of Polarization of the Incident Beam

It is implicit in the discussion of Sec. II that the polarization of the first-scattered beam at the position of the hydrogen target is purely transverse in the R geometry and that the polarization vector lies exactly in the second scattering plane. We expect small deviations from both of these conditions for the following reasons.

Assume for simplicity that the cyclotron pole faces and the median planes of the magnetic fields of the quadrupole and wedge magnets all lie exactly in the horizontal plane. It is possible for the mean direction of protons striking the first target in the cyclotron to deviate from the horizontal because of slight magnet imperfections. Since the betatron vertical-oscillation frequency at the radius of the first target is small compared to the cyclotron frequency, we can consider such an effect as equivalent to a tilt of the plane of the mean orbit away from the horizontal; this tilt may be a few tenths of a degree. Consider now the first scattered beam. It may also deviate slightly from the horizontal because of inexact vertical placement of magnets and slits; we did in fact observe inclinations of a few tenths of a degree. Either of these effects means that the first-scattered plane is not exactly horizontal, and consequently that the polarization has a horizontal component. Although the polarization at the first scattering is exactly transverse, the bending of the beam in the fringe and focusing fields will cause the horizontal component to precess relative to the momentum vector.

Following the above, we may expect that the polarization at the $T_2(R)$ position has a small longitudinal component. It is then evident from Eq. (1) that, in the R geometry, we detect in fact terms in the polarization which depend on the A parameter. In the A geometry the value of the angle χ will be slightly in error. It is apparent, however, that this is a very small effect; the longitudinal component of polarization in the R geometry should not be more than 0.003. Since the resulting errors in the determination of R and A are much smaller than the statistical errors, we do not take them into account.

C. Errors in the Scattering Angle

Several effects contribute to the uncertainty in effective scattering angle; uncertainty in the position of the beam center at the hydrogen target, inaccurate alignment of the polarimeter, and uncertainty in the correction for kinematic and range effects. We estimate each of these errors to be equivalent to about 3 minutes in the scattering angle. We therefore take the uncertainty in c.m. scattering angle to be about 30 min.

D. Consistency of the Data

We have examined the results obtained in different runs in order to see if they are statistically consistent. In the case of the R data, the differences between different runs are perfectly consistent with assuming no experimental error at all. The results for e_A/e_C are also consistent, except for one datum point, the point at 50° in run 2. Since this result differs by about four standard deviations from the mean of the results of runs 1 and 3, we follow the usual practice of discarding it.

It is of course well known that systematic errors cannot be detected, therefore we cannot include such error in the result.

VII. ANALYSIS OF THE RESULTS

A. Present Experimental Situation

As was explained in the introduction, the Rochester group intends to complete the measurement of the basic

set of quantities $d\sigma/d\omega$ (unpolarized cross section), P (polarization), and the triple scattering parameters D, R, and A at 213 Mev in the hope that a unique solution for the scattering matrix (or equivalently, a unique phase shift solution) can be found at this energy. We have available at present, in addition to the results for R and A described in this paper, the earlier measurement of polarization[16] and preliminary results[17] for the triple scattering parameter D at 30° and 60°. The cross section was measured some years ago,[18] but for a somewhat different energy—240 Mev. A remeasurement of the cross section at 213 Mev is in progress.[19]

B. Phase Shift Analysis

Although it is evident that as yet we have an incomplete set of data at 213 Mev, a considerable effort has already been made to search for phase shift solutions. MacGregor and Moravcsik[20] have obtained encouraging results by using a modified form of analysis which restricts the number of the theoretical parameters. Their procedure is now well known. They attribute the effect of high angular-momentum partial waves ($l \geq 5$) entirely to the one-meson exchange contribution, which can be predicted exactly. The remaining parameters (eight phase shifts and one coupling parameter) are then to be determined from the experiments. They have published solutions found in this manner, based on preliminary data excluding any knowledge of D. Even with such crude information, they found only four acceptable phase shift sets, which they labeled by the letters a, b, c, and d. A later analysis,[21] which included measurements of D at 30° and 60° c.m.,[17] showed that solution b is now favored strongly over solutions a and c, while solution d has disappeared. On a statistical basis, however, the result is somewhat disturbing; whereas the expected value of the fitting parameter χ^2 is 29, the value corresponding to solution b is 64.3, and to solutions c and a, 143.3 and 236.5, respectively. Thus even the most favorable solution does not give an acceptable fit to the data. Moravcsik and MacGregor have noted, however, that the three large-angle points for the cross section contribute 17 to the χ^2 sum, which is certainly excessive. If one remembers also that the cross section refers to a significantly different energy than do the other parameters, one may hope that this is the cause of the difficulty. Recent additional D measurements[22] and an analysis of the photodisintegration of the deuteron[23] seem to rule out all solutions except b. This solution is very similar to solution 1 of Stapp, Ypsilantis, and Metropolis.[3] The results of solution b are given in the first row of Table VIII, and are shown in Figs. 9 and 10.

C. Phenomenological Models

As better data on proton-proton scattering become availabe, phenomenological potential models such as those originally proposed by Signell and Marshak[24] and Gammel and Thaler[25] are put to more and more severe tests. The phenomenological approach is more ambitious than the phase shift analysis at one energy since the predictions of the model must, if successful, fit data over a wide range of energy. While the early attempts were only partially successful for energies greater than 150 Mev, recent refinements by Bryan[26] (a more careful treatment of the spin-orbit potential as well as of the short-distance behavior of the tensor and central potentials) resulted in considerable improvement. Even more recently, Saylor *et al.*[27] have succeeded in matching data quite well over the range of 40 to 310 Mev using what they call the boundary condition model. We list the calculated phase shifts from the latter model for 210 Mev in the second row of Table VIII and show the predictions for R and A in Fig. 9 and 10. The similarity between this result and the solution of MacGregor and Moravcsik is indeed striking.

D. Outlook

The rather encouraging results of the partial wave analysis described in Sec. VII (B) lead one to inquire as to what additional refinements are desirable both in the experimental and in the analytical procedures.[28]

First it is evident that the scattering experiments must be continued until a phase shift analysis yields a single solution for which the χ^2 sum is statistically acceptable. One must then obtain an error matrix (i.e., determine the precision with which each phase shift is known) from which one can decide whether the precision

[16] E. Baskir, E. Hafner, A. Roberts, and J. Tinlot, Phys. Rev. **106**, 564 (1957).

[17] K. Gotow and E. Heer, Phys. Rev. Letters **5**, 111 (1960).

[18] C. L. Oxley and R. D. Schamberger, Phys. Rev. **85**, 416 (1952); O. A. Towler, *ibid.* **85**, 1024 (1951).

[19] A. Konradi and J. Tinlot (private communication).

[20] M. H. MacGregor and M. J. Moravcsik, Phys. Rev. Letters **4**, 524 (1960).

[21] M. H. MacGregor, M. J. Moravcsik, and H. P. Noyes (private communication); we are grateful to these authors for giving us results of their analysis prior to publication. The computations were based on the preliminary data reported at Rochester. (See Reference 15).

[22] K. Gotow, B. Lobkowicz, and E. Heer (private communication).

[23] G. Kramer, Phys. Rev. Letters **5**, 439 (1960).

[24] P. S. Signell and R. E. Marshak, Phys. Rev. **109**, 1229 (1958).

[25] J. L. Gammel, R. Christian, and R. S. Thaler, Phys. Rev. **105**, 311 (1957); J. L. Gammel and R. S. Thaler, *ibid.* **107**, 291 (1957).

[26] R. Bryan, Nuovo cimento **16**, 895 (1960).

[27] D. P. Saylor, R. A. Bryan, and R. E. Marshak, Phys. Rev. Letters **5**, 266 (1960).

[28] The MacGregor and Moravcsik[20] analysis was performed using a computer program which required using σ, P, D, R, and A as input information, whereas to be correct in our case, one should use the ratio e_A/e_C rather than A. This minor objection will presumably be overcome in future calculations.

of the experiments should be further improved. One should then consider the appearance of solutions at different energies, as has recently been done by Breit[29] and by Stapp *et al.*[30] If the behavior of the individual phase shifts is statistically unreasonable, one may suspect systematic errors in one or more sets of experiments. In anticipation of such problems, we therefore plan to extend our program somewhat beyond the complete set defined earlier.[31] Although this amounts to overdetermining the scattering matrix, it may be helpful in increasing our confidence concerning the contributions of systematic errors, and should also increase the general precision of the phase shift analysis.

ACKNOWLEDGMENTS

We wish to thank Professor A. Roberts for contributions to the early stages of the experiment, A. Konradi for his help in taking data, Professor R. E. Marshak, Dr. M. Moravcsik, and Dr. H. P. Noyes for helpful discussions concerning the analysis of the results.

[29] G. Breit, *Proceedings of the London Conference on Nuclear Forces and the Few Nucleon Problem* (Pergamon Press, New York, 1960), p. 23; G. Breit, M. H. Hull, Jr., K. E. Lassiler, and K. D. Pyatt, Jr. Phys. Rev. **120**, 2227 (1960).

[30] H. P. Stapp, M. J. Moravcsik, and H. P. Noyes, *Proceedings of the 1960 Annual International Conference on High-Energy Physics at Rochester*; (Interscience Publishers, New York, 1960), p. 28.

[31] A measurement of the triple scattering parameter R' is in preparation. K. Gotow, B. Lobkowicz, and E. Heer (private communication).